Available online at www.sciencedirect.com
SCIENCE DIRECT®
Pergamon
Cement and Concrete Research 34 (2004) 321–328
CEMENT AND CONCRETE RESEARCH

Assessment of permeation quality of concrete through mercury intrusion porosimetry

Rakesh Kumar[a,*], B. Bhattacharjee[b]

[a]Bridges Division, Central Road Research Institute, Delhi Mathura Road, New Delhi 110 020, India
[b]Department of Civil Engineering, Indian Institute of Technology Delhi, New Delhi 110 016, India

Received 11 April 2003; accepted 11 August 2003

Abstract

Permeation quality of laboratory cast concrete beams was determined through initial surface absorption test (ISAT). The pore system characteristics of the same concrete beam specimens were determined through mercury intrusion porosimetry (MIP). Data so obtained on the measured initial surface absorption rate of water by concrete and characteristics of pore system of concrete estimated from porosimetry results were used to develop correlations between them. Through these correlations, potential of MIP in assessing the durability quality of concrete in actual structure is demonstrated.

Keywords: Permeation quality; Concrete; Initial surface absorption rate; Pore system; Mercury porosimetry; Durability

1. Introduction

Durability of structural concrete is mainly dependent on its permeation quality. Therefore, assessment of durability quality of concrete plays an important role in the performance evaluation of structural concrete. Most often, durability quality of concrete in structure is assessed through in situ tests, such as initial surface absorption test (ISAT) [1,2], water absorption on drilled core [2,3], Figg's water and air permeability tests [3], 'CLAM' tests that include sorptivity and permeability tests and cover crete test [4]. Mainly, the permeation quality of surface concrete is assessed by these tests, and the results are expressed in terms of a permeation index. Most of the deterioration processes in concrete involve permeation of fluids from its surrounding. The ingress of fluid to interior of concrete takes place through its pore systems [5–7]. This ingress is followed by physical/chemical changes in the internal structure of concrete leading to its deterioration. For instance, the ingress of CO_2 in moist concrete through its pore leads to carbonation while the ingress of moisture as well as oxygen in concrete contaminated with chloride causes corrosion of reinforcement. Hence, permeation indices render themselves as measures of durability quality. A permeation index is again dependent on the pore system characteristics of concrete. The most important characteristics of pore system of concrete are its porosity and pore-size distribution. In fact, these pore system characteristics play the most decisive role in deterioration processes of concrete [5–9]. Therefore, durability quality of structural concrete can be assessed indirectly from the knowledge of its pore system characteristics. However, to enable the above, it is necessary to establish a correlation between the pore system characteristics and the durability quality of concrete. Durability quality of concrete can be classified in terms of low, average or high permeability/absorption based on the value of measured permeation index [2–4]. Hence, through a relationship between a suitable permeation index and the pore system characteristics mentioned, a reliable correlation between durability quality of concrete and pore system characteristics can be established. The porosity and pore-size distribution can be easily determined through mercury intrusion porosimeter test. Therefore, by establishing a correlation between the chosen permeation index with porosity and pore-size distribution of concrete, it is possible to assess the durability quality of concrete indirectly from the mercury intrusion porosimetry

* Corresponding author. Tel.: +91-11-26314424; fax: +91-11-26830480.
E-mail address: rakesh_crri@hotmail.com (R. Kumar).

0008-8846/$ – see front matter © 2003 Elsevier Ltd. All rights reserved.
doi:10.1016/j.cemconres.2003.08.013

(MIP) results in terms of low, average or high permeation/absorption. Thus, MIP can be used as an additional methodology for assessment of durability quality of concrete in structure.

Among the tests mentioned earlier, ISAT is the simplest. This test has been successfully used in past to assess the durability quality of concrete [2–4,10–13]. Further, this method provides four permeation indices such as water absorption rate at 10, 30, 60 and 120 min. These permeation indices are used for classifying the concrete durability quality in terms of low, medium or high permeation/absorption. Hence, in this work, these four initial surface absorption rates were used to correlate results of (an extensive experimental study) initial surface absorption rates of water with porosity and a characteristic pore size of the pore system of concrete. By using correlation so obtained, a method of classifying the permeation quality of concrete based on its pore structure characteristics has been suggested. The suitable statistical approaches as suggested in literature [14–16] were extensively used for justification of the correlation obtained.

2. Experimental study

2.1. Mix proportions and experimental factors

Durability of structural concrete strongly depends upon its pore system characteristics, which is ultimately function of water–cement ratio. Considering the practical limits of water–cement ratios (0.38–0.65) for workable concrete without water-reducing agent, six concrete mixes were designed so as to ensure adequate variation in permeation as well as durability quality of concrete. Same ordinary Portland cement was used throughout this investigation. Similarly, throughout the investigation, same land-quarried local sand confirming to zone II of British Standard and potable laboratory tap water were used as fine aggregate and mixing water, respectively. Crushed 20-mm maximum size of graded aggregate of quartzite origin was used as coarse aggregate. Coarse aggregate had negligible water absorption. To ensure maximum variation in pore structural characteristics of concrete, two modes of compaction, namely, compaction through poker vibrator and manual compaction through tamping rod, were adopted in the experimental programme. In this study, the modes of compaction adopted are referred as V.C. and H.C., respectively. Details about the mix proportions, beam specimen cast and modes of compaction adopted, etc., are presented in Table 1. The fact that degree of hydration, that is, the age, curing, exposure to aggressive environment, affect strength, permeation quality and pore system characteristics of concrete were kept in mind while planning this study. Thus, further variation in permeation quality, porosity and pore-size distribution of concrete was ensured by adopting different age, curing period and exposure to acidic water as variable factors. Therefore, two test ages (28 and 84 days), two levels of curing period (that is, moist curing for 1 and 27 days) and two levels of exposure conditions (namely, exposure to open air and exposure to acidic environment of pH 4–5, to simulate acid rain condition) were adopted to cause variation in quality of concrete (Table 2). The details of the samples prepared are given subsequently.

Table 1
Concrete mix proportions; mix designation and beam cast from each mix

Mix proportions	Mix designation	Beam cast and mode of compaction	
C:S:CA:W		V.C.	H.C.
1:2.5:5.1:0.65	Mix 1	1	2
1:2.2:4.2:0.56	Mix 2	3, 5, 7, 9	4, 6, 8
1:1.8:3.9:0.51	Mix 3	10	11
1:1.5:3.6:0.46	Mix 4	12	–
1:1.3:3.2:0.42	Mix 5	13	14
1:1.1:2.7:0.36	Mix 6	15, 17, 18	16, 19

C = cement, S = sand, CA = coarse aggregate, W = water.

2.2. Concrete specimens

ISAT is conducted in situ on the structural elements for durability assessment. Hence, concrete beam specimens of dimensions $100 \times 200 \times 1000$ mm were cast, and the durability quality of concrete was assessed through ISAT. Because mercury intrusion porosimetry can be performed only on small samples due to restricted dimensions of the penetrometer cell, hence, small cores of required dimensions were drilled out from the concrete beam specimens to assess the pore system characteristics of the concrete.

2.3. Casting, curing and exposure conditions

The method of casting, curing and exposure conditions, etc., for the beam specimens were kept similar to that described in details in an earlier paper by the authors [12]. However, the details of concrete mix proportions, mix designation, beam cast and means of compaction adopted, etc., are shown in Table 1. Details of age of concrete beams, curing, exposure conditions, initial surface absorption rates of water at different time, etc., are presented in Table 2.

2.4. Testing

2.4.1. Initial surface absorption test

This test was conducted on the concrete beam specimens as per the procedure laid in BS 1881: Part 5 [2]. On each of the beams, this test was conducted at three to four points, and the rates of absorption of water at 10, 30, 60 and 120 min from the start of test were noted. The detail of the same has been also reported in earlier paper [12]. The results of this test are presented in Table 2.

Table 2
Age and curing, exposure condition, in situ strength and ISA rates of water by concrete in beams

Beam number	Curing (days)	Exposure		Age at testing days	In situ strength (MPa)	Initial surface absorption rates (ml/m^2 s)			
		Condition	Duration after curing (days)			10 min	30 min	60 min	120 min
1	27	normal	0	28	18.3	0.322	0.193	0.139	0.085
2	27	normal	0	28	15.5	0.273	0.180	0.134	0.081
3	27	normal	0	28	28.4	0.124	0.077	0.048	0.044
4	27	normal	0	28	24.0	0.198	0.134	0.087	0.058
5	27	acidic	90	118	27.5	0.110	0.067	0.047	0.038
6	27	acidic	90	118	23.7	0.256	0.169	0.140	0.116
7	1	normal	0	28	26.8	0.302	0.180	0.134	0.087
8	1	normal	0	28	23.2	0.539	0.360	0.260	0.240
9	27	normal	90	90	29.7	0.100	0.041	0.022	0.017
10	27	normal	0	28	30.3	0.070	0.045	0.035	0.025
11	27	normal	0	28	30.3	0.312	0.192	0.134	0.064
12	27	normal	0	28	35.3	0.116	0.033	0.020	0.016
13	27	normal	0	28	40.3	0.048	0.016	0.013	0.010
14	27	normal	0	28	37.7	0.054	0.032	0.023	0.020
15	27	normal	0	28	43.2	0.048	0.033	0.021	0.016
16	27	normal	0	28	35.3	0.084	0.064	0.052	0.035
17	27	acidic	90	28	42.5	0.033	0.024	0.018	0.017
18	1	normal	90	118	39.3	0.122	0.076	0.046	0.035
19	1	normal	90	118	38.5	0.130	0.074	0.048	0.035

2.4.2. Mercury intrusion porosimetry

MIP is widely adopted for the study of porosity and pore-size distribution of cement-based composites such as cement paste, mortar and concrete [5–9,13,17–35]. A number of factors affect the MIP results. Most important among them are the method of sampling, sample conditioning, rate of pressure application, maximum intrusion pressure applied, assumed values of contact angle and surface tension of mercury [13,18,24,28,31,32]. Because samples used in MIP test are small and average result must be representative of the parent structural concrete, therefore, the number of samples required to obtain relevant MIP results within the limits of desirable accuracy, the suitable method for sample collection, the suitable form of the sample and the suitable rate of pressure application were arrived at through a preliminary experimental investigation. Suitable method for sample conditioning (oven drying) contact angle and surface tension values of mercury were adopted from available literature [32–36]. In addition, certain minor factors, such as expansion of sample cell under pressure, differential mercury compression, sample compression and hydrostatic head of mercury, also affect the MIP results to a limited extent, and effects of these factors were neglected [13,18,31].

2.4.2.1. Sample preparation and conditioning. MIP test was performed on small-cored samples taken out from the beams in order to generate relevant information about the pore system characteristics of the concrete. The procedure of this test is described in details somewhere else [31]. Six small cores, 25 mm in diameter and 15–25 mm in length, were drilled from the concrete beams and used as the samples for MIP tests. The small cores were dried in an oven at 105–110 °C for 24 h and stored in a desiccator until testing. Preliminary investigation carried out has revealed that the sample in the form of small core is the most suitable form of the sample that can be used for assessing pore system characteristics of concrete through MIP [13,31]. Modification of the concrete pore system if any, due to coring, would affect the results of every sample in a similar manner.

2.4.2.2. Testing. Testing was performed on a Quanta chrome Autoscan-33 mercury porosimeter having a pressure range from sub-ambient to 33,000 psi. The contact angle and the surface tension of mercury were assumed to be 117° [13,18,24,29] and 0.484 N/m [13,18,24,29], respectively, for the oven-dried samples. Consequently, assuming the cylindrical pores, the Washburns equation yields

$$r = 63{,}750/P$$

where P is the applied pressure in psi and r is in nm. With this pressure (33,000 psi), the smallest size of pore in to which mercury can be intruded is 2 nm. Thus, the pressure is sufficient to ensure intrusion of mercury in all the capillary pores, as the reported radius of smallest size capillary pore is 5 nm. However, majority of the gel pores would remain non-intruded. The sample cell fitted with the base cell of capacity 17.7 cm^3 was used throughout the experiment. Six numbers of samples have been reported to be sufficient in order to obtain the result within ± 15% variation [29]. Hence, six numbers of samples were used to ensure adequate accuracy of the MIP results representing particular concrete. All tests were performed at a constant moderate scanning rate indicated by a graduation mark of 5 on a 0–10 scale of machine knob [13,29,31]. The rate of scanning has negligible effect on

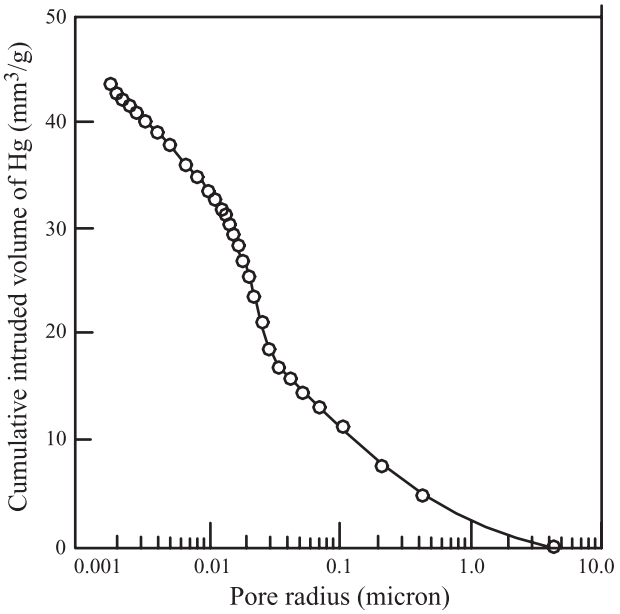

Fig. 1. A typical pore-size distribution curve of H.C. concrete Mix 5.

measured pore-size distribution of concrete [31]. To obtain representative pore-size distribution curve for the concrete in a particular beam, the results of six porosimetry data were averaged. For this purpose, the intruded volumes of mercury for all the six samples at a particular radius of the pore were averaged to obtain average intruded volume of mercury at that pore radius. This procedure was repeated at a large number of pore radii to generate the resulting average pore-size distribution curve. A typical pore-size distribution curve for Mix 5 for H.C.-designated concrete at the age of 28 days is shown in Fig. 1. The nature of this pore-size distribution curve is similar to those reported in literature [37]. In situ strength of concrete in all beams was estimated according to the procedure stated in an earlier paper [12,38]. The in situ strength was determined through core test. Cores of 75-mm diameter and 100-mm length were drilled out from the beam to estimate the strength of concrete in the beam. The in situ strength of the concrete in beams after the exposure period is given in Table 2. From the intrusion curves of six samples collected from a beam, an average representative intrusion curve was obtained for concrete in each beam. The porosity of the concrete (corresponding to 33,000 psi intrusion pressure) for each of the six samples taken from a beam was calculated using the individual cumulative intrusion volume and the relevant mass measurements for a sample, and averaged. Averaged porosity of concrete in each of the beam was thus obtained.

3. Pore system characteristics

Interconnected porosity [39–43] and pore-size distribution are the most important pore system characteristics influencing the durability performance of concrete. The porosity is well defined while pore sizes can be described through a pore-size distribution curve. Thus, for establishing a correlation between durability performance and pore-size characteristics, it is necessary to express the pore sizes in terms of a single effective pore radius. Two effective pore radii suggested in literature as defined below are used in the empirical correlation presented. The test was performed on each sample and two cycles of intrusion–extrusion curves were obtained. The relevant pore structure characteristics of concrete such as equivalent pore radius (r_e) and mean distribution radius (r_m) was calculated by using the data of above said representative pore-size distribution curve obtained for the concrete in beams. The estimation of equivalent pore radius (r_e) was done by adopting the Eq. (1) suggested by Reinhardt and Gaber [32], and the mean distribution radius (r_m) was estimated using the Eq. (2) suggested by Atzeni et al. [7] given below:

$$r_e^2 = \frac{\int \frac{dv}{d(\log r)} r^2 d(\log r)}{\int \frac{dv}{d(\log r)} d(\log r)} \quad (1)$$

where dv is the volume of pores corresponding to radius r.

$$\ln r_m = \frac{\sum_{i=1}^{n} V_i \ln r_i}{\sum_{i=1}^{n} V_i} \quad (2)$$

where V_i is the pore volume corresponding to radius r_i, and r_m is the mean distribution radius of pore.

The equivalent pore radius (r_e) is defined as a uni-sized pore radius of a concrete medium that would lead to the same permeability of concrete when considered a medium having a series of cylindrical parallel pores of varying radii and calculated by using Eq. (1). The mean distribution pore radius is defined as the mean pore size and is the weighted average, weighted with respect to the volume of pores at the corresponding pore radius. The significant difference between the equivalent pore radius and mean distribution radius is that the equivalent pore radius is the square root of weighted average radius squared, whereas the mean radius is the simple weighted average. Both radii are weighted with respect to the corresponding volume. In equivalent pore radius, a greater importance to larger size pores is given. The calculation of equivalent pore radius (r_e) and mean distribution radius (r_m) of concrete was done using data of first as well as second intrusion curves of intrusion–extrusion curves.

3.1. Relationship between ISA rate of water and pore system characteristics of concrete

3.1.1. Theoretical background

Initial surface absorption rate of water by concrete is the rate of flow of water into concrete per unit area at a stated

interval from the start of the test at a constant applied head and temperature [1–3]. The initial rate of absorption of water has been reported to vary with t^{-n} where t stands for the time and n is silting factor [1–3]. The values of n ranges from 0.3 to 0.7. The rate of absorption in one-dimensional flow is shown to be proportional to $t^{-1/2}$ after assuming a parallel tubes model of porous media by Martys and Ferraris [44]. Same model cannot be applied for initial surface absorption rate in concrete slab or beam, but the dependence of ISAT results on t^{-n} is thus confirmed. The permeability of material depends upon its porosity and pore system characteristics. The rate of flow of water under the suction and gravity head in unsaturated concrete can be assumed to be governed by generalized Darcy's law [45]. The material property that is involved in the Darcy's law is the moisture content dependent permeability (K) of the material. The rate of absorption, which is again related to the rate of flow, thus can be assumed to be dependent on the permeability of material. Martys and Ferraris [44] demonstrated that one-dimensional absorption rate is dependent on permeability, pore radius, surface tension, contact angle, etc. Modeling of relationship between the initial surface absorption rate and the pore structure characteristics is complex and thus for a simple empirical relationship following form was assumed $I_t = f(K, t^{-n})$, where I_t is the initial surface absorption rate at time t, and K is permeability. Reinhardt and Gaber [32] model for permeability of concrete has the equation $K = ap^m r_e^2$, where m is a factor that represents relative influence of porosity p and depends up on the interconnectivity of the pores, a is an empirical coefficient. Through mercury porosimetry, only interconnected porosity is measured; thus, when p estimated from mercury porosimetry is used, m can be assumed to be one (as a first approximation). Thus, I_t can be expressed as $I_t = f(pr_e^2, t^{-n})$, where p is in fraction and r_e is in μm. Regression model of this form is thus presented below using the data generated.

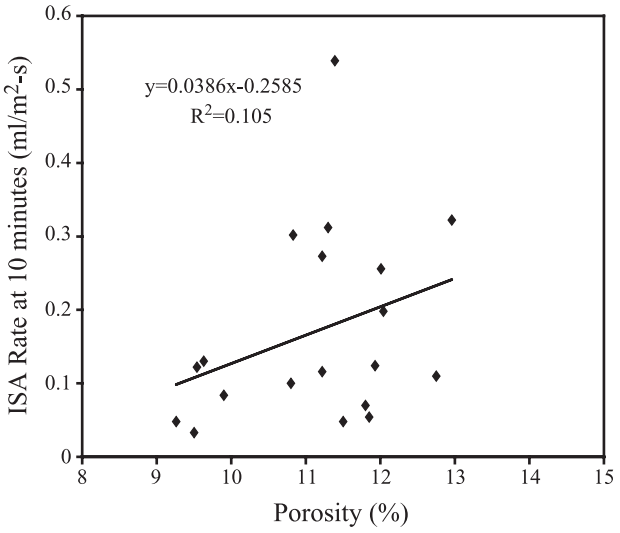

Fig. 2. ISA rate at 10 min vs. porosity.

Table 3
Equation and correlation coefficient of curves

Equation	Coefficient of correlation (c_r)
$I_{10} = 6.82(pr_e^2)^{1.659}$	72
$I_{30} = 4.01(pr_e^2)^{1.643}$	71
$I_{60} = 2.87(pr_e^2)^{1.666}$	70
$I_{120} = 1.82(pr_e^2)^{1.509}$	68

3.1.2. Regression models

The permeability of material depends upon free pores rather than trapped pores or enclosed pores. In mercury porosimetry test, the first intrusion curve of first cycle of intrusion–extrusion curves represents free as well as trapped pore-size distribution, while the second intrusion curve represents the distribution of free pores only [17]. Hence, in this investigation, the relevant results obtained from first and second intrusion curve of MIP test were tried. The plot (Fig. 2) of initial surface absorption rate of water by concrete against it porosity demonstrated a very poor correlation (32%) between them. This shows that initial surface absorption rate is not only dependent on porosity but also on some other characteristics of pore system such as pore-size distribution. The plots of initial surface absorption rates against equivalent pore radius and mean distribution radius both exhibited a linear trend with a negative intercept at ISA rate axis indicating an increase in ISA rate with increase in pore size. The plot of ISA rate against the product of porosity and equivalent pore radius showed a linear trend with negative intercept on ISA rate axis. This negative intercept implies that up to a minimum value of porosity; surface absorption rate by concrete is zero. This seems to be less probable compared to a situation in which a zero surface absorption corresponds to zero porosity. An attempt to obtain a relationship of the form $I_t = ap^m r_e^2$ was also unsuccessful as the estimated correlation coefficient was extremely low (34%). Although the above form of the equation passes through the origin, this form of equation does not describe the above variation much better.

A similar exercise as above with pr_e^2 values computed from second intrusion data of porosimetry was also carried out. It was observed that pr_e^2 values calculated from the second intrusion data show lower correlation coefficient than that obtained for the data of pore system characteristics obtained for first cycle of intrusion curve when plotted against ISA rates. Further, the nature of the curves observed was similar with a negative intercept on the ISA rate axis. Thus, it may be true that free pores govern permeability of concrete for saturated flow rather than total pores including both free and entrapped pores; however, the surface absorption rate of water by unsaturated concrete depends on both the types of pores. Further, in both cases, the best-fit equations do not pass through the origin; thus, simple $I_t = Ap^m r_e^2$ form of equation was discarded. A relationship of the form of $I_t = A(pr_e^2)^m$ was found to describe the above variation much better. The above equation also passes through the origin. To arrive at the

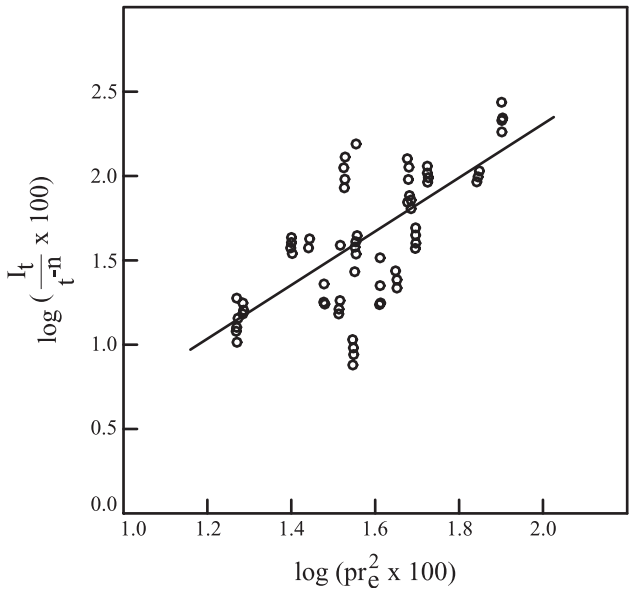

Fig. 3. $\log[(I_t/t^{-n})100]$ vs. $\log(pr_e^2 \times 100)$.

above equation, log of initial surface absorption rate at 10, 30, 60 and 120 min was plotted against log of pr_e^2. The resultant equations along with the coefficient of correlation are given in Table 3. It is observed from Table 3 that the exponent m varies from 1.509 to 1.666 (within $\pm 7\%$ of the mean). This variation of m does not follow any systematic pattern with time. However, the constant A decreases systematically with time. Therefore, A is time dependent and assumed to be related to t^{-n}. Thus, a more general equation involving time can be written as

$$I_t = Bt^{-n}(pr_e^2)^m \tag{3}$$

Table 4
Forms of equation and correlation coefficient of curves

Forms of equation			
$y = a_{11} + b_{11}x$		$y = a_{11}x$	
Equation	Coefficient of correlation (c_r)	Equation	Coefficient of Correlation (c_r)
$I_{10} = 0.85(pr_m^2 \times 10) + 0.003$	76	$I_{10} = 0.96 (pr_m^2 \times 10)$	76
$I_{30} = 0.56(pr_m^2 \times 10) + 0.008$	79	$I_{10} = 0.60 (pr_m^2 \times 10)$	79
$I_{60} = 0.42(pr_m^2 \times 10) + 0.004$	78	$I_{10} = 0.45 (pr_m^2 \times 10)$	78
$I_{120} = 0.34(pr_m^2 \times 10) - 0.005$	81	$I_{10} = 0.34 (pr_m^2 \times 10)$	81

In this equation, B, n, and m are the unknown coefficients. A logarithmic transformation of both sides results in

$$\log I_t = \log B - n\log t + m\log(pr_e^2) \tag{4}$$

The multiple linear regression on the above transformed data as shown in Fig. 3 results in the following equation

$$I_t = 1.84t^{-0.48}(pr_e^2)^{1.52} \tag{5}$$

or

$$I_t \approx 1.84t^{-0.5}(pr_e^2)^{1.5} \tag{6}$$

or

$$I_t \approx 1.84t^{-0.5}p^{1.5}r_e^3 \tag{7}$$

The estimated coefficient of correlation for the above equation is 70%. All unaccounted factors are built in the constant B.

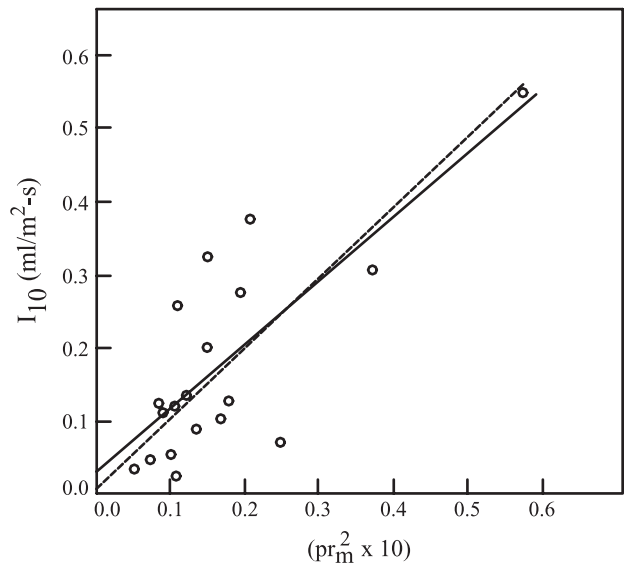

Fig. 4. A typical ISA vs. $pr_m^2 \times 10$.

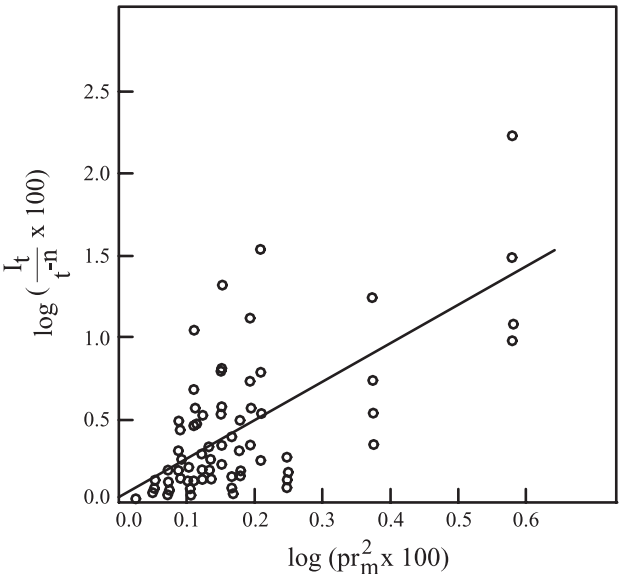

Fig. 5. $\log[(I_t/t^{-n})100]$ vs. $\log(pr_m^2 \times 100)$.

Table 5
Permeation quality of concrete through ISAT and MIP results

ISA rate at	Permeation quality of concrete								
	Low			Average			High		
	ISA rate (ml/m^2/s)	pr_e^2	pr_m^2	ISA rate (ml/m^2/s)	pr_e^2	pr_m^2	ISA rate (ml/m^2/s)	pr_e^2	pr_m^2
10 min	<0.25	<0.558	<0.272	0.25–0.50	0.058–0.982	0.272–0.543	>0.50	>0.982	>0.854
30 min	<0.17	<0.610	<0.311	0.17–0.35	0.61–0.853	0.311–0.64	>0.35	>0.853	>0.640
60 min	<0.10	<0.540	<0.258	0.1–0.2	0.54–0.879	0.258–0.516	>0.20	>0.879	>0.516
120 min	<0.07	<0.532	<0.253	0.07–0.15	0.532–0.879	0.253–0.541	>0.15	>0.543	>0.879
Mean		<0.560	<0.274		0.560–0.898	0.274–0.560		>0.898	>0.560

p is in %, r_e and r_m in μm.

3.2. Relationship between ISA rate of water and mean distribution pore radius of concrete

In order to investigate relationship between ISA rate of water and mean distribution pore radius of concrete curves between I_t and pr_m^2 was plotted for four different time value, that is, 10, 30, 60 and 120 min, respectively. A typical curve for this is shown in Fig. 4. The form of equation and coefficient of correlation of the curves are given in Table 4. These curves exhibit a linear relationship between I_t and pr_m^2; hence, m is unity in these relationship. From the Table 4, it is obvious that there is a marginal reduction in coefficient of correlation by forcing the curve to pass through origin. The generalization of ISA results for time of measurement yields in the following empirical equation

$$I_t = \ddot{a}t^{-0.5}pr_m^2 \quad (8)$$

where $\ddot{a}$ is a constant and other symbols have the same meaning as defined earlier.On estimation of $\ddot{a}$ in the similar manner as earlier, the above equation becomes

$$I_t = 2.8t^{-0.5}pr_m^2 \quad (9)$$

It may be noted that this equation is obtained by forcing the line to pass through origin (Fig. 5), and its coefficient of correlation is 80%. It is interesting to note that when r_m is used instead of r_e, a better and simple correlation results. This may be due to greater influence given to the larger pores in the estimation of equivalent pore radius.

4. Permeation quality of concrete based on ISAT and MIP tests results

From the knowledge of range of ISA rates and pr_e^2 or pr_m^2 values of concrete, the concrete may be classified as low, average or high absorption quality as given in Table 5. The study of above table reveals that on the basis of results of porosimetry test, permeation quality of concrete can be assessed. The Eq. (9) exhibits a better correlation than Eq. (7). Further, this equation is also simpler. Considering the overall predictability, one may prefer Eq. (9) rather than Eq. (7).

5. Conclusions

The following conclusions can be drawn from this experimental investigation:

1. The permeation quality of concrete can be assessed on the basis of the knowledge of porosity and pore system characteristics of concrete such as equivalent pore radius and mean distribution pore radius of the concrete obtained through MIP results.
2. The relationship involving mean distribution pore radius of the pores yields a better correlation than that involving equivalent pore radius.
3. MIP can be used as an additional method for assessing the permeation quality of concrete.

Acknowledgements

The kind permission of the Director Central Road Research Institute, New Delhi, India, to publish this research paper is highly acknowledged.

References

[1] J.H. Bungey, Testing of Concrete in Structures, 2nd ed., Chapman and Hall, New York, 1989.
[2] BS 1881: 1970, Methods of Testing Concrete: Part 5. Methods of Testing Hardened Concrete for other than Strength, BSI, London.
[3] A.D. Campbell, H. Roper, Concrete Structures: Materials, Maintenance and Repair, Longman Scientific and Technical Co., UK, 1996.
[4] P.A.M. Basheer, A brief review of methods for measuring the permeation properties of concrete in-situ, Buildings and Structures, vol. 99, Institution of Civil Engineers, London, 1993, pp. 74–83.
[5] E.J. Garboczi, Permeability, diffusivity and microstructural parameters: A critical review, Cem. Concr. Res. 20 (4) (1990) 503–514.
[6] O. Valenta, Durability of concrete, 2nd RILEM Symposium, Prague, Mater. Struct. 3 (17) (1970) 333–345.
[7] C. Atzeni, L. Massidda, U. Sanna, Effect of pore size distribution on strength of hardened cement pastes, Proceedings of the First Interna-

tional RILEM Congress on Pore Structure and Material Properties, Paris, Chapman & Hall, London, 1987, pp. 195–202.
[8] G.M. Därr, U. Ludwing, Determination of permeable porosity, Mat. Struct. 6 (33) (1973) 185–190.
[9] F.S. Rostasy, R. Weib, G. Wiedemann, Changes of pore structure of cement mortars due to temperature, Cem. Concr. Res. 10 (2) (1980) 157–164.
[10] S. Kelham, A water absorption test for concrete, Mag. Concr. Res. 40 (2) (1988) 106–110.
[11] W.F. Price, P.B. Bamforth, Initial surface absorption of concrete: examination of modified test apparatus for obtaining uni-axial absorption, Mag. Concr. Res. 45 (1) (1993) 4–17.
[12] R. Kumar, B. Bhattacharjee, Correlation between initial surface absorption rate of water and in-situ strength of concrete, Indian Concr. Journal 76 (4) (2002) 231–235.
[13] R. Kumar, Strength and permeation quality of concrete through mercury intrusion porosimetry, PhD thesis, Department of Civil Engineering, Indian Institute of Technology Delhi, India, 1997.
[14] G. Chengju, Some statistical points in predicting strength of concrete by empirical methods, Proceedings of 2nd International RILEM Symposium, Paris, E & FN SPON, Chapman & Hall, London, 1991, pp. 461–472.
[15] I. Miller, J.E. Freund, Probability and Statistics for Engineer, Prentice-Hall of India, Private Limited, New Delhi, India, 1981.
[16] W. Mendenhall, D.D. Wackerly, R.L. Scheaffer, Mathematical Statistics with Applications, 4th ed., PWS-KENT Publishing, Boston, MA, 1990.
[17] P. Parcevaux, Pore size distribution of Portland cement slurries at very early stages of hydration (influence of curing, temperature and pressure), Cem. Concr. Res. 14 (3) (1984) 419–430.
[18] S. Diamond, A critical comparison of mercury intrusion porosimetry and capillary condensation pore size distribution of Portland cement pastes, Cem. Concr. Res. 11 (5) (1971) 531–545.
[19] M. Sadegzadch, C.L. Page, R.S. Kettle, Surface microstructure and abrasion of concrete, Cem. Concr. Res. 17 (4) (1987) 581–590.
[20] N. Hearn, R.D. Hooton, Sample mass and dimension effects on mercury intrusion porosimetry results, Cem. Concr. Res. 22 (5) (1992) 970–980.
[21] M. Moukwa, P.C. Aïtcin, The effect of drying on cement pastes pore structure as determined by mercury porosimetry, Cem. Concr. Res. 18 (5) (1988) 745–752.
[22] A. Auskern, W. Horn, Capillary porosity in hardened cement paste, J. Test. Eval. 1 (1) (1973) 74–79.
[23] F. Metz, D. Knöfel, Systematic mercury porosimetry investigations on sand stones, Mat. Struct. 25 (1) (1992) 127–136.
[24] R.A. Cook, K.C. Hover, Experiments on contact angle between mercury and hardened cement paste, Cem. Concr. Res. 21 (6) (1991) 1165–1175.
[25] P.K. Mehta, Concrete: Structure, Properties and Materials, Prentice Hall, New Jersey, 1995.
[26] M. Maage, Frost resistance and pore size distribution in bricks, Mat. Struct. 17 (101) (1984) 345–350.
[27] D. Manhoman, P.K. Mehta, Influence of pozzolanic slag and chemical admixtures on pore size distribution and permeability of hardened cement pastes, Cem., Concr. Aggreg. 3 (1) (1981) 63–67.
[28] S. Lowell, J.E. Sheilds, Powder Surface Area and Porosity, Chapman & Hall, London, 1984.
[29] A.I. Laskar, R. Kumar, B. Bhattacharjee, Some aspects of evaluation of concrete through mercury intrusion porosimetry, Cem. Concr. Res. 27 (1) (1997) 93–105.
[30] R. Kumar, B. Bhattacharjee, Mercury intrusion porosimetry: A technique to study durability of concrete, Proceeding of Seventh NCB International Seminar on Cement and Building Materials, NCCBM, New Delhi, India, 2000, Part VIII, pp. B23–26.
[31] R. Kumar, B. Bhattacharjee, Study on some factors affecting the results in the use of MIP method in concrete research, Cem. Concr. Res. 33 (3) (2003) 417–424.
[32] H.W. Reinhardt, K. Gaber, From pore size distribution to an equivalent pore size distribution of cement mortar, Mat. Struct. 23 (133) (1990) 3–15.
[33] D.N. Winslow, S. Diamond, A mercury porosimetry study of the evaluation of porosity in Portland cement, J. Mater. 5 (3) (1970) 564–585.
[34] D.H. Bager, E.J. Sellevold, Mercury porosimetry of hardened cement paste, the influence of particle size, Cem. Concr. Res. 5 (2) (1975) 171–177.
[35] U. Schneider, U. Diederichs, Detection of crack by mercury penetration measurement, in: F.H. Wittmann (Ed.), Fracture Mechanics of Concrete, Elsevier Science Publishers, Amsterdam, 1983, pp. 207–222.
[36] A.K. Suryavanshi, R.N. Swamy, Influence of penetrating chlorides on the pore structure of structural concrete, Cem., Concr. Aggreg. 20 (2) (1998) 169–179.
[37] J.J. Beaudoin, J. Marchand, Pore structure, in: V.S. Ramachandran, J.J. Beaudoin (Eds.), Handbook of Analytic Techniques in Concrete Science and Technology, Principles, Techniques, and Applications, Noyes Publication, New Jersey, 1999, pp. 529–628.
[38] R. Kumar, B. Bhattacharjee, Strength, porosity and pore size distribution of concrete, Cem. Concr. Res. 33 (1) (2003) 155–164.
[39] A.J. Katz, A.H. Thompson, Quantitative prediction of permeability in porous rock, Phys. Rev., B 34 (11) (1986) 8179–8181.
[40] A.J. Katz, A.H. Thompson, Prediction of rock electrical conductivity from mercury injection measurements, J. Geophys. Res. 92 (B1) (1987) 599–607.
[41] A.S. EL-Dieb, R.D. Hooton, Evaluation of the Katz–Thompson model for the estimating the water permeability of cement-based materials from mercury intrusion porosimetry data, Cem. Concr. Res. 24 (3) (1994) 443–455.
[42] R.D. Hooton, Permeability and pore structure of cement pastes containing fly ash, slag, and silica fume, in: G. Fronhnsdorff (Ed.), Blended Cements, ASTM STP 897, American Society for Testing and Materials, Philadelphia, 1986, pp. 128–143.
[43] J.P. Ollivier, M. Massat, Permeability and microstructure of concrete: a review of modelling, Cem. Concr. Res. 22 (2–3) (1992) 503–514.
[44] N.S. Martys, C.F. Ferraris, Capillary transport in mortars and concrete, Cem. Concr. Res. 27 (5) (1997) 747–760.
[45] C. Hall, Water movement in porous buildings materials: 1. Unsaturated flow theory and its applications, Build. Environ. 12 (1) (1977) 117–125.